Microplastic ingestion induces changes in coelomocyte composition of *Eisenia fetida*

Johanna K. Fritsche[1,6], Max V. R. Döring[2,6], Anika Mauel[3], Jürgen Senker[3], Heike Feldhaar[2,4,7,*], Ruth Freitag[1,5,7,*], Valérie Jérôme[1],

[1] Process Biotechnology, Faculty of Engineering Sciences, University of Bayreuth, Bayreuth, Germany

[2] Animal Population Ecology, Animal Ecology I, University of Bayreuth, Bayreuth, Germany

[3] Inorganic Chemistry III and Northern Bavarian NMR Centre, University of Bayreuth, Bayreuth, Germany

[4] Bayreuth Center of Ecology and Environmental Research (BayCEER), Bayreuth, Germany

[5] Bayreuth Center for Molecular Biosciences (BZMB), Bayreuth, Germany

[6] These authors contributed equally

[7] These authors jointly supervised this work

Address: University of Bayreuth, 95440 Bayreuth, Germany

Corresponding authors*: ruth.freitag@uni-bayreuth.de, heike.feldhaar@uni-bayreuth.de

ORCID numbers

Johanna Katharina Fritsche: 0009-0009-6344-8164

Max V. R. Döring: 0009-0002-3672-4820

Anika Mauel: 0000-0003-0776-4532

Jürgen Senker: 0000-0002-7278-7952

Heike Feldhaar: 0000-0001-6797-5126

Ruth Freitag: 0000-0002-6569-9137

Valérie Jérôme: 0000-0001-6492-2168

Abstract

The earthworm *Eisenia fetida* is a widely used model organism for environmental toxicity assessment, including microplastic particles (MPP). Impacts of MPP at the organismic level have been extensively documented. Effects on the cellular level and in particular the immune system of *E. fetida* are less well understood. Here we exposed earthworms outside soil for six days to food pellets containing 10% (w/w) pure polystyrene (PS) MPP (25 – 75 µm) or PS MPP supplemented with 0.5% (w/w) of the antioxidant Irgafos ($PS_{Irgafos}$). Immune cells (coelomocytes) were isolated from *E. fetida* using a non-invasive extrusion method, and their number, viability, and subpopulation distribution (amoebocytes and eleocytes) were assessed by flow cytometry. Husbandry outside soil was found to generally increase propensity for apoptosis in particular of amoebocytes with little difference between experimental setups. The total number of extruded cells was not affected by MPP, while coelomocyte viability was significantly reduced. $PS_{Irgafos}$ ingestion further decreased the number of living cells per mg fresh weight. *Ex vivo* analysis of coelomocyte viability confirmed an enhanced toxicity of $PS_{Irgafos}$ compared to PS. Our findings show that MPP and their additives cause physiological changes and alter immune cell distribution, posing potential risks to soil invertebrates.

Key Words

Annelida

Polystyrene

Irgafos

Additive

Coelomocytes

Flow Cytometer

Graphical Abstract

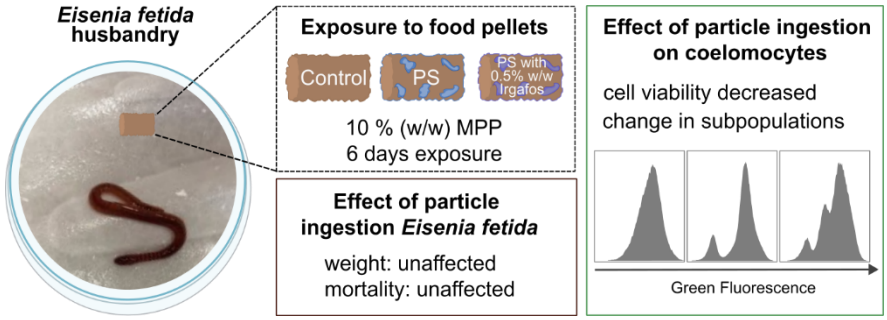

1. Introduction

Plastic pollution increasingly burdens the environment globally. Plastic debris is known for adverse effects on organisms. It can lead to entanglement (Kühn & Van Franeker, 2020) and may result in starvation following ingestion (Santos et al., 2021). Plastic products in addition typically contain various additives, including flame retardants and antioxidants (van Oers et al., 2012). These additives substantially enhance chemical and physical properties of polymers and are therefore incorporated into environmentally relevant plastic products such as agricultural mulch films (Reay et al., 2025), packaging materials (Hermabessiere et al., 2020), and textiles (Y. Chen et al., 2022). Since additives are not covalently bound to the polymer matrix (Iftikhar et al., 2024), these substances may leach into the environment (Li et al., 2019; Reay et al., 2025). Additives have been shown to induce adverse effects on organisms, including higher mortality in *Daphnia magna* exposed to the antioxidant tris(2-chloroethyl)phosphate (Iftikhar et al., 2024). Moreover, in the environment, plastics inevitably fragment and degrade over time into particles smaller than 1 mm, commonly referred to as (secondary) microplastic particles (MPP) (*DIN EN ISO 24187*, 2024). Terrestrial ecosystems are estimated to contain high amounts of MPP (estimated worldwide 1.5 to 6.6 million tons) (Earth Action, 2023; Horton et al., 2017; Kedzierski et al., 2023). Once in the soils, MPP can alter soil properties, e.g. lower the pH (Lozano et al., 2021), reduce water infiltration capacity (Qiu et al., 2022), and affect the physiology and ecological functions of soil organisms (M. Liu et al., 2023; Qiu et al., 2022).

Earthworms, such as *Eisenia fetida*, play a major role in organic matter fragmentation, nutrient cycling, and the improvement of soil physical conditions (Blouin et al., 2013; Edwards & Arancon, 2022). Since earthworms ingest soil contaminated with MPP and are in direct contact with these particles through their skin, MPP have the potential to compromise earthworm physiology through multiple mechanisms (e.g. injuries to the setae and epidermis after exposure to low-density polyethylene particle in soil (Y. Chen et al., 2020; J. Liu et al., 2022)). Moreover, ingestion

of PS MPP injured the digestive tract of *E. fetida* (Jiang et al., 2020). Exposure to polyethylene fragments decreased reproductive fitness (Yang et al., 2023) and induced oxidative stress at both transcriptomic and metabolic levels (K. Chen et al., 2022). Various MPP types were also shown to alter the microbiome composition of earthworms (Holzinger et al., 2023; Papazlatani et al., 2024). Common plastic additives may lead to additional adverse effects. For example, the flame retardant tetrabromobisphenol A, has been shown to elevate hydroxyl radical levels in *E. fetida*, as measured in earthworm homogenate (Xue et al., 2009).

The immune system of *E. fetida* plays a central role in protecting the organism against pathogenic challenges and in counteracting oxidative stress (Engelmann et al., 2002; Homa et al., 2016). Coelomocytes, the earthworm's main immune cells, mediate pathogen recognition as well as phagocytosis and clearance, thus serving as key effectors of innate immunity (Engelmann et al., 2002). Coelomocytes are free-circulating cells in the coelomic fluid. In response to stress, coelomic fluid is released through dorsal pores by the earthworms. This process enables the isolation of coelomocytes without the need to sacrifice or dissect the animal and reduces carry over of non-coelomic cells (Homa et al., 2008; Irizar et al., 2014). Coelomocytes encompass at least two distinct subpopulations: amoebocytes and eleocytes. Amoebocytes are macrophage-like cells, approximately 2 µm in diameter, responsible for several defense mechanisms, including phagocytosis (Adamowicz & Wojtaszek, 2001; Bodó et al., 2018; Engelmann et al., 2016). Amoebocyte numbers are known to decrease with stress, e.g. after dermal exposure to immunostimulants (Homa et al., 2016). Eleocytes are approximately 10 times larger (approximately 20 µm) and characterized by a highly granular cytoplasm (Adamowicz & Wojtaszek, 2001). They are responsible for producing and secreting immune-active molecules (Mazur et al., 2011). Amoebocytes originate from the mesenchymal lining of the coelom (Kurek et al., 2007), eleocytes originate from the chloragogen tissue and store high amounts of riboflavin, which is responsible for their characteristic green autofluorescence (Koziol et al.,

2006). Amoebocytes display only minimal autofluorescence, facilitating flow cytometric separation of the two populations (Manna et al., 2022). Flow cytometry analyses have demonstrated that amoebocyte abundance increased 2.5-fold in *Eisenia andrei* after exposure to immunostimulants such as lipopolysaccharides (mimicking bacterial pathogens) compared to untreated earthworms (Homa et al., 2013, 2016). In contrast, the stored riboflavin has been suggested as biomarker of soil metal contamination. Plytycz et al. (2009) demonstrated, e.g., that heavy metal exposure markedly reduces riboflavin-derived autofluorescence in coelomocytes. Iron exposure reduces coelomocyte autofluorescence without reducing cell numbers (Du et al., 2020). Regarding the two coelomocyte subtypes, Irizar et al. (2015) showed that eleocytes have lower toxicity thresholds than amoebocytes, in particular regarding metal exposure. *In vitro* experiments with isolated coelomocytes showed that PS nanoparticles (100 nm) are internalized by coelomocytes and subsequently reduce cell viability, increase ROS production, and induce apoptosis (Shi et al., 2024). However, in that study it was not differentiated between eleocytes and amoebocytes.

Here, we investigate whether the ingestion of polystyrene MPP, with or without Irgafos 168 as additive, induces adverse effects in *E. fetida* and whether systemic responses manifest as detectable changes at the immune cell level. We established an experimental setup in which earthworms were kept on moistened filter paper in Petri dishes and fed food pellets prepared from standardized diet spiked with the respective MPP. This experimental setup limited dermal exposure and ensured particle ingestion. The uptake of MPP was confirmed using fluorescence-labelled PS particles under otherwise identical experimental conditions. The effects of MPP uptake on the coelomocytes were investigated in terms of cell number, cell viability, and coelomocyte subpopulation distribution. To complement our *in vivo* experiments and directly assess the cellular response, we evaluated the metabolic activity of the extruded coelomocytes *ex vivo*.

2. Materials and Methods

If not otherwise indicated, Greiner Bio-One (Frickenhausen, Germany) and Thermo Fisher Scientific (Schwerte, Germany) were used as suppliers for cell culture materials and chemicals. Leibovitz-15 medium and Ultraglutamine™ I was obtained from Lonza (Lonza Group Ltd., Basel, Switzerland). Foetal calf serum (FCS), penicillin-streptomycin solution, tetracycline and amphotericin B, 4',6-diamidin-2-phenylindol (DAPI) and 3-(4,5-dimethyl-2-thiazolyl) 2,5-diphenyl-2 H tetrazolium bromide (MTT) were from Sigma Aldrich (Taufkirchen, Germany). Gentamycin was from Biowest (Nuaillé, France). HEPES ((4-(2-hydroxyethyl)-1-piperazineethanesulfonic acid) was from Biochrom AG (Berlin, Germany).

2.1. Production and characterization of microplastic particles

Polystyrene particles (PS), PS particles with 0.5% w/w Irgafos 168 ($PS_{Irgafos}$), and fluorescent rhodamine B labelled PS particles (PS_{red}, λ_{max} = 544 nm) were produced and characterized in-house by members of the CRC 1357 consortium (Project Z01) to ensure strict control over the MPP composition. A detailed description of how the particles were produced (Method S1) and characterized by dynamic light scattering (Method S2) can be found in the supplementary information. The particles had a size range between 20 - 75 µm, with mean diameters of 60.21 µm (PS), 57.0 µm (PS_{red}), and 70.4 µm ($PS_{Irgafos}$). Residual monomer content was quantified by liquid NMR (Method S3, Fig. S1-S2, Table S1).

2.2. Earthworm husbandry

E. fetida earthworms were kept in a climate chamber at constant conditions of 20 °C and 70% atmospheric moisture under a 12:12 h light:dark cycle. They were reared in wormeries (Wurmfarm 42 × 42 × 60 cm, vidaXL, Venlo, Netherlands) containing a mixture 75% worm cultivation soil (Regenwurm-Zuchterde, SUPERWURM GmbH & CO. KG, Vettweiß, Germany) and 25% coconut fibres (Humusziegel.de, Wörmlitz, Germany). The soil moisture was adjusted

155 weekly to be around 60% (w/w). Earthworms were fed once a week with specialized worm food
156 (SPEZIAL-Wurmfutter, SUPERWURM GmbH & Co. KG, Vettweiß, Germany).

157 **2.3. Preparation of microplastic spiked food pellets**

158 The food pellets were made by mixing worm food (SPEZIAL-Wurmfutter, SUPERWURM GmbH &
159 Co. KG, Vettweiß, Germany) with equal parts MilliQ water, after which small pellets were formed
160 (diameter: about 0.5 cm; weight: 0.5 ± 0.015 g). For the MPP exposure, we replaced 10% (w/w) of
161 the worm food (50 mg per pellet) with MPP. All pellets were freshly prepared once a week, after
162 which they were stored them at 4 °C until further use.

163 **2.4. Earthworm exposure to food pellets**

164 The controlled exposure of the earthworms to MPP required their husbandry outside soil while
165 providing sufficient humidity. Therefore, all incubation steps were performed in a wet chamber
166 consisting of a Petri dish (Ø: 10 cm) containing 0.75 g cotton wool (dm-drogerie markt GmbH +
167 Co. KG, Karlsruhe, Germany), saturated with MilliQ water (excess water was drained). Further, a
168 moistened filter paper (ROTILABO 601A, Carl Roth GmbH & Co. KG, Karlsruhe, Germany) was
169 laid on top of the cotton wool. Finally, another moistened filter paper was placed in the lid to
170 provide additional humidity. It was not necessary to re-moisten the filter papers during the
171 experiments. First the weight of adult *E. fetida* (i.e. with clitellum) was recorded (weight 250 - 450
172 mg) before they were exposed to MPP-spiked food pellets in these wet chambers, which were
173 placed in the climate chamber (20 °C, 70% atmospheric moisture, 12:12 h light:dark cycle).

174 **2.5. Evaluation of MPP uptake**

175 To confirm ingestion of MPP via food pellets, we conducted a feeding trial with fluorescently
176 labelled MPP (PS_{red}) and assessed the presence of PS_{red}-derived fluorescence within the digestive
177 tracts of the earthworms by fluorescence microscopy. Prior to feeding, 60 adult earthworms

were allowed to defecate for 24 h in Petri dishes, prepared as described above, to ensure gut clearance. After defecating, each earthworm was transferred to a new wet chamber, along with one food pellet. In 50% of the cases the pellets consisted solely of earthworm food (mock), while the others contained earthworm food supplemented with 10% (w/w) PS_{red}. Wet chambers were placed in the climate chamber (20 °C, 70% atmospheric moisture, 12:12 h light:dark cycle). Every day, earthworm mortality was assessed, and they were examined using a Leica M205 FCA fluorescence stereo microscope (Leica Microsystems GmbH, Wetzlar, Germany) equipped with a Leica DBC6200 camera and the Leica Application Suite X software (version 3.8.2.27713), image acquisition time: 250 ms.

2.6. Exposure of *E. fetida* to microplastic particles with and without additive

To investigate the effects of MPP on coelomocytes, we allowed 12 individuals to defecate for 24 h, weighed them, and afterwards randomly assigned four each to one of three treatments (n = 4 per treatment): mock treatment (worm food pellets), PS (worm food pellets containing 10% (w/w) PS particles), and $PS_{irgafos}$ (worm food pellets containing 10% (w/w) PS particles with 0.5% Irgafos 168). After six days, the earthworms were allowed to defecate for 24 h in fresh petri dishes to prevent contamination with faeces during the subsequent isolation of coelomocytes and were weighed again. This procedure was replicated a total of seven times, leading to a total number of 72 earthworms with 24 earthworms per treatment. One earthworm of the PS treatment was lost during the exposure period, resulting in a sample size of n = 23 in this group.

We additionally analysed whether the husbandry outside soil in general affects the earthworms' coelomocyte abundance, viability, and subtype distribution. Therefore, earthworms were incubated for 24 h in the wet chamber (n = 8), representing the minimal period required for defecation to reduce microbial contamination and enable subsequent *ex vivo* cell culture (hereafter called control).

202 **2.7. Coelomocyte isolation**

203 Following 24 h of defecation, earthworms were briefly rinsed with sterile MilliQ water, gently dried
204 with laboratory paper towels, and then transferred into pre-weighted sterile empty 15 mL conical
205 tubes. Earthworm fresh weight (fw) was calculated according to equation 1:

206 Earthworm weight prior to extrusion = total tube weight – empty tube weight (1)

207 Coelomocytes were extruded from the worms by a method adapted from (Eyambe et al., 1991).
208 Briefly, into each 15 mL conical tube containing one earthworm we added 3 mL of ice-cold (4 °C)
209 extrusion solution (71.2 mM NaCl, 5.0 mM EGTA, 50.4 mM guaiacol glyceryl ether, 100 U/mL
210 penicillin/streptomycin, 50 µg/mL gentamycin, 60 µg/mL tetracycline, 2.5 µg/mL amphotericin,
211 5% (v/v) absolute ethanol, pH 7.3) and the tube kept on ice for 3 minutes. Coelomocyte release
212 was indicated by an increased turbidity of the extrusion solution. Afterwards, extruded
213 coelomocytes were transferred into 50 mL conical tubes filled with 9 mL ice-cold (4 °C) M-HBSS
214 (Hank's Balanced Salt Solution) adapted after Diogéne et al (1997) and Hendawi et al. (2004)
215 (58.5 mM NaCl, 5.3 mM KCl, 0.4 mM KH_2PO_4, 0.3 mM Na_2HPO_4, 4.1 mM $NaHCO_3$, 0.4 mM
216 Na_2SO_4, 10 mM HEPES, 5.5 mM glucose, 100 U/mL penicillin/streptomycin, 50 µg/mL
217 gentamycin, 60 µg/mL tetracycline, 2.5 µg/mL amphotericin B, pH 7.3). Cells were collected by
218 centrifugation (530 *g,* 10 min, 4 °C). The supernatant was discarded, and the cell pellet was
219 mechanically dislocated, resuspended in 5 mL fresh ice-cold (4 °C) M-HBSS buffer and
220 centrifuged again (530 *g,* 10 min, 4 °C). After discarding the supernatant, the cell pellet was
221 resuspended in 1 mL ice-cold (4 °C) M-HBSS buffer. An initial cell count with a Luna-FL™ dual
222 fluorescence cell counter (Logos Biosystems) was performed. 18 µL of the coelomocyte
223 suspensions were stained with Acridine Orange/Propidium Iodide Stain (Logos Biosystems) to
224 assess total cell number.

2.8. Isolation of coelomic fluid as cell culture supplement

For *ex vivo* coelomocyte cultivation, coelomic fluid (CF) was used as cell culture supplement. Previous studies have demonstrated that supplementation with CF supports the *ex vivo* cultivation of primary intestinal cells isolated from *E. fetida,* maintaining a cell viability >85% over 144 h cultivation (Riedl et al., 2021). For isolation of CF, earthworms were briefly rinsed first with tap water, followed by sterile MilliQ water, then gently dried with laboratory paper towels and anesthetized by incubation at -20 °C for 10 minutes. Earthworms were then dissected longitudinally beginning behind the clitellum and proceeding from anterior to posterior. CF was captured with a capillary, collected in an Eppendorf tube and stored on ice. CF was centrifuged at 3990 *g* for 5 minutes to remove cellular components. The supernatant was collected and diluted 1:10 in ice-cold (4 °C) M-HBSS, sterile filtered through a 0.2 µm syringe filter and stored on ice until use.

2.9. *Ex vivo* coelomocyte cultivation

Freshly isolated coelomocytes were cultivated in Leibovitz medium, supplemented with 10% (v/v) FCS, 2% (v/v) CF, 100 U/mL penicillin/streptomycin, 50 µg/mL gentamycin, 60 µg/mL tetracycline, 2.5 µg/mL amphotericin, further referred to as L10 culture medium. Cells were cultivated at 20 °C, 95% relative humidity and without additional CO_2 gassing. Under these conditions, the coelomocytes remained viable, with viability >80% for up to one week, as established in preliminary experiments. No proliferation was observed, however, cell numbers remained stable. The medium was not replaced during this period to minimize cell loss.

2.10. Flow cytometric analysis of coelomocytes

Cells were analysed with a Cytoflex S flow cytometer from Beckman Coulter (Brea, USA) equipped with 405 nm, 488 nm, and 561 nm lasers. Isolated coelomocytes were suspended in 1 mL ice-cold (4 °C) M-HBSS buffer. Dead cells were counterstained with 1 µg/mL DAPI, a

membrane permeable dye (Atale et al., 2014; Sauvat et al., 2015). Forward scatter (FSC), side scatter (SSC), green fluorescence (488 nm laser, 525 nm filter) and DAPI fluorescence (405 nm laser, 450 nm filter) were recorded. The entire sample was used for the measurement, and data were collected from at least 40,000 events.

Flow cytometry (FC) data were analysed using FlowJo (version 10.10.0, Tree Star, Standford University, CA, USA, 2018). DAPI fluorescence intensity over all coelomocyte subpopulations was used to assess cell viability and the appearance of a sub-G1 peak, indicating apoptotic cells (Fig. 1A). For further analysis, cells were initially evaluated by scatter properties (FSC/SSC, linear scale) to select the coelomocyte population (Fig. 1B, Gate: “Coelomocytes”) and to exclude aggregates and apoptotic cells.

The number of viable coelomocytes per mg fw of the earthworms was calculated according to equation 2:

$$living\ coelomocytes\ per\ mg\ fw\ =\ number\ of\ coelomocytes\ per\ mg\ fw\ \times (1\ -\ dead\ cells) \quad (2)$$

where dead cells represent the proportion of DAPI stained cells (between 0 and 1) in the entire cell population. 0 equals no dead cells and 1 means all cells are dead.

For further analysis dead cells were excluded to focus on viable cells (Fig. 1C, Gate “viable”). Within this gate, green fluorescence intensities in the histograms were used to identify coelomocyte subpopulations based on riboflavin content: (riboflavin^{Dim}; fluorescence intensity 450–7K), riboflavin^{Bright}; fluorescence intensity 35K -1.5M) (Fig. 1D). Green fluorescence and SSC properties of viable cells were used to distinguish amoebocytes (low SSC, dim fluorescence) from eleocytes (high SSC, bright fluorescence) (Mazur et al., 2011)(Fig. 1E).

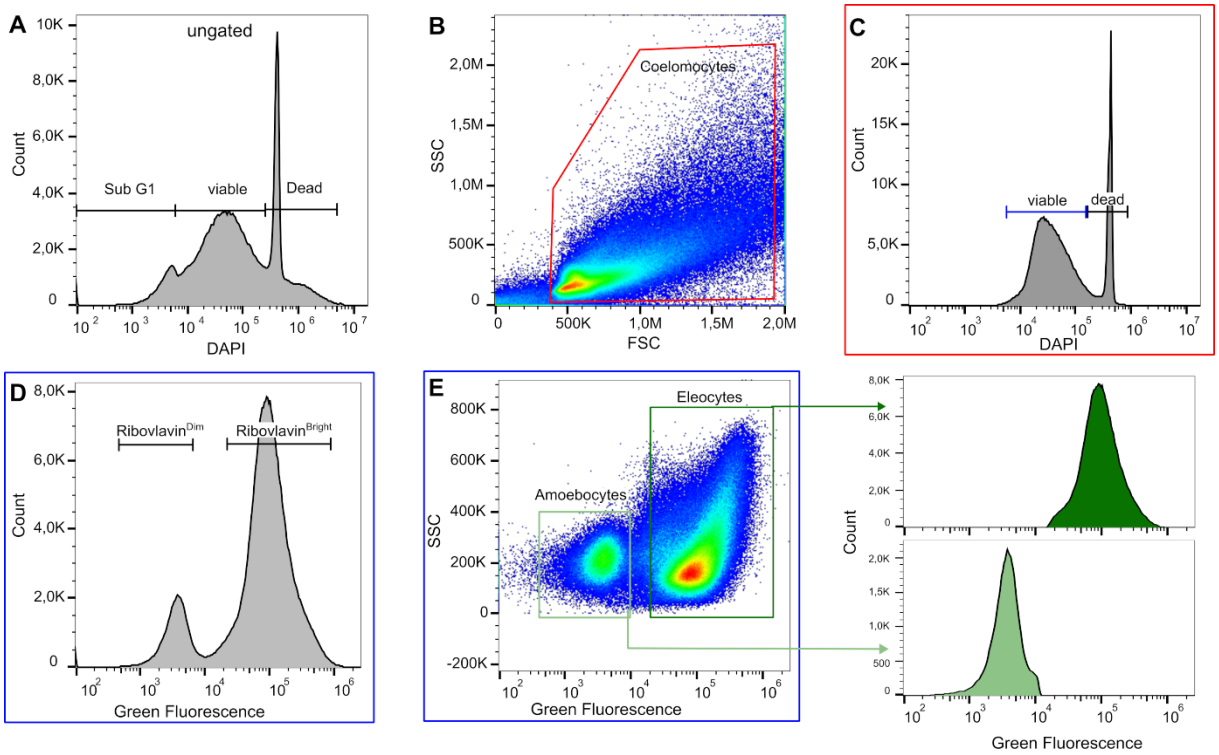

Fig. 1 Representative gating strategy for flow cytometry analysis. (A) DAPI fluorescence of the "ungated" sample enables the detection of a "SubG1" peak, indicating apototic cells. (B) Initial gating of cells was performed in the FSC vs. SSC dot plot to define the total cell population. (C) viable and dead DAPI stained cells were identified in the "coelomocytes" gate and selected in the DAPI histogram. D) Coelomocyte subpopulations in the viable gate (DAPI histogram) according to their riboflavin content were identified (riboflavin^{Dim}; fluorescence intensity 450–7K, riboflavin^{Bright}; fluorescence intensity 35K -1.5M). (E) In the green fluorescence vs SSC plot amoebocytes and eleocytes were distinguished based on their green auto-fluorescence (gate "viable" in DAPI histogram (C)).

2.11. MTT Assay

Coelomocyte viability was assessed *ex vivo* by MTT assays performed as previously described for *E. fetida* intestinal cells (Riedl et al., 2021), with minor modifications. Briefly, coelomocytes from eight individuals were isolated and 450,000 cells were seeded in 700 µL L10 medium. Cells were exposed to PS or $PS_{Irgafos}$ at concentrations from 1 to 250 µg/mL (1, 10, 25, 50, 75, 125, 250 µg/mL) for 24, 72, and 144 h. Cells cultivated in the absence of MPP served as negative control, cells treated with 0.1% (v/v) Triton X100 for 24 h served as positive control. After the respective cultivation time, 70 µL of freshly prepared MTT stock solution was added (10 mg/mL in M-HBSS, sterile filtered) to a final concentration of 1 mg/mL. After 24 h of incubation, cells were harvested by centrifugation (530 *g*, 10 min) and the supernatant was discarded. Cells were lysed in 700 µL DMSO for 2 min. The suspension was aliquoted into six wells of a 96 well plate. The absorbance

at 580 nm (reference wavelength 670 nm) was measured using a TECAN GENios Pro plate reader (Tecan Austria GmbH, Gröding, Austria). The metabolic activity of cells was calculated according to equation 3:

$$metabolic\ activity\ [\%] = \frac{Abs580_{sample} - Abs580_{blank}}{Abs580_{control} - Abs580_{blank}} * 100 \quad (3)$$

where $Abs580_{sample}$ is the mean absorbance of the test sample, $Abs580_{control}$ is the mean absorbance of the negative control (0 µg/mL MPP) at the same time point, and $Abs580_{blank}$ the absorbance of DMSO.

2.12. Statistical analysis

All statistical analyses were conducted in R (version 4.3.1 (R Core Team, 2023)). We analysed the earthworms' weight at the start and end of our six-day feeding trial, and cellular responses after MPP exposure using linear mixed models (lmm) with treatment as a fixed factor and the starting day as a random intercept. The models were created using the package *lme4* (version 1.1-35.1(Bates et al., 2015)). We checked model assumptions such as normal distribution of the residuals with the *DHARMa* package (version 0.4.7 (Hartig, 2022)). If the ANOVA from the *car* package (version 3.1-3 (Fox & Weisberg, 2019)) showed a significant p-value ($p < 0.05$), we performed a two-sided Dunnett post-hoc test with Benjamini-Hochberg correction from the *multcomp* package (version 1.4-29 (Hothorn et al., 2008)) for pairwise comparisons. The number of cell subpopulations in our flow cytometry data was compared among treatments using a chisq-test. Subsequent pairwise comparisons of the subpopulation compositions between treatments were conducted using chisq-tests. Since we are mainly interested in the effects of MPP on coelomocytes, we did not include the controls in our models or chisq-tests. Metabolic activity of coelomocytes after *ex vivo* PS exposure was compared between different MPP concentrations and time points using a Kruskal-Wallis rank sum test and subsequent pairwise Dunn's post-hoc test (version 1.3.6 (Dinno, 2024)). The *ex vivo* analysis was repeated separately

316 with $PS_{Irgafos}$. The bar- and boxplots were generated using the packages *ggplot2* (version 4.0.0
317 (Wickham, 2016)) and *dplyr* (version 1.1.4 (Wickham et al., 2023)) and arranged with *ggpubr*
318 (version 0.6.2 (Kassambara, 2023)).

319 ## 3. Results and Discussion

320 ### 3.1. Uptake of MPP by *E. fetida*

321 To determine whether earthworms are feeding on the pellets in our setup and thus ingest MPP,
322 30 earthworms per treatment were exposed to either mock or PS_{red}-spiked food pellets (Fig. 2).
323 The first group was used to determine the auto-fluorescence of the tissue. Whereas no
324 autofluorescence of the earthworms themselves was detected with our settings (Fig. 2B), PS_{red}
325 were visible as brightly red particles, within the intestinal tract (Fig. 2D). Nine of the 30
326 earthworms (30%) exposed to PS_{red} had ingested MPP after two days. By day four, 23 (77%) had
327 done so. Over six days, all 30 individuals exposed to PS_{red} had ingested the MPP (Table 1). In
328 contrast, no red fluorescence was detected in earthworms of the mock group, indicating minimal
329 tissue autofluorescence of *E. fetida*.

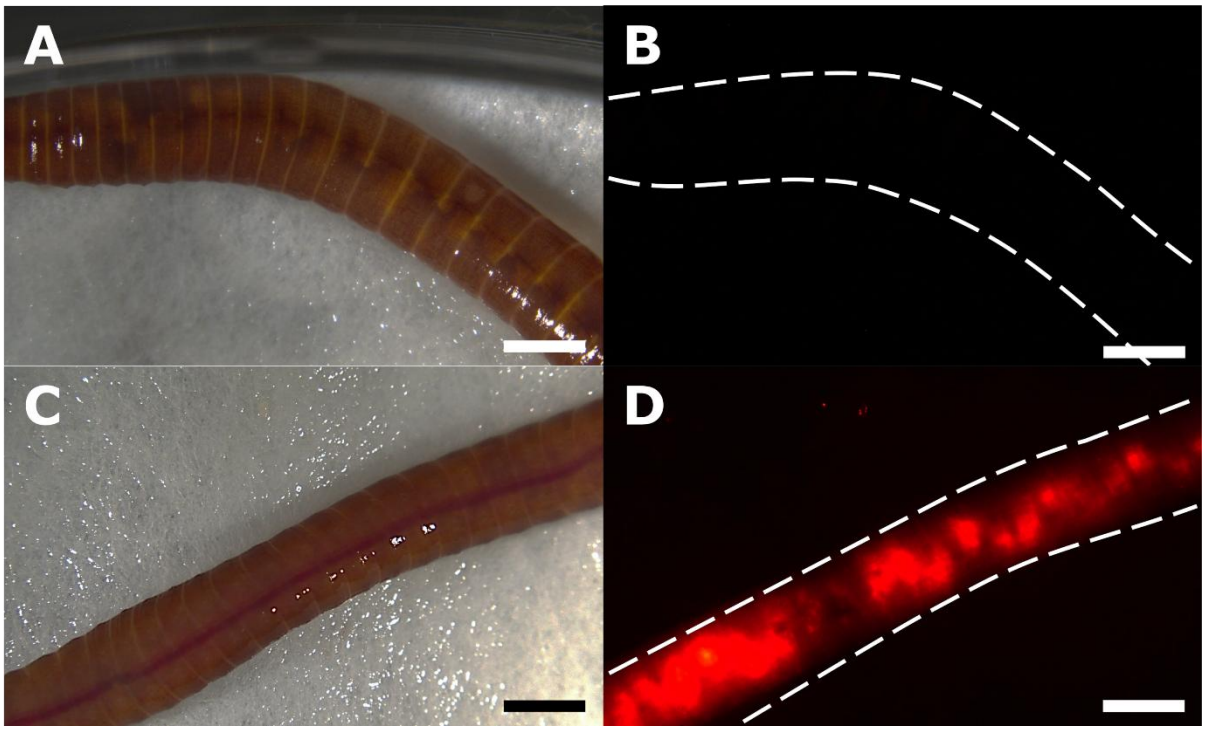

Fig. 2 Representative images of *E. fetida* displaying the uptake of microplastic particles. (A, B) *E. fetida* fed with pellets consisting of worm food only (mock) or (C, D) worm food mixed with 10% w/w PS_{red}. (A, C) View of the earthworm using light microscopy. (B, D) View of the earthworm using fluorescence stereo microscopy. White dashed lines mark the position of the earthworm in B and D. Scale bar: 1 mm.

Table 1 Ingestion of fluorescent MPP (PS_{red}) by the earth worms throughout the feeding trial.

Day	Individuals that ingested MPP for the first time	Sum of individuals that ingested MPP for the first time	Total number of individuals with ingested MPP
1	0 (0%)	0 (0%)	0 (0%)
2	9 (30%)	9 (30%)	9 (30%)
3	15 (50%)	24 (80%)	20 (67%)
4	6 (20%)	30 (100%)	23 (77%)
5	0 (0%)	30 (100%)	22 (73%)
6	0 (0%)	30 (100%)	9 (30%)

Earthworms fed with a mock food pellet (i.e. without PS_{red}) are not shown, since no MPP was found in their gut.

In contrast to the commonly used method of gut dissection to validate uptake (e.g. (Xiao et al., 2022)), our non-invasive approach enabled the repeated assessment of MPP ingestion and accumulation over time within the intestine of the same individual.

On average, earthworms retained the PS_{red} MPP for three days. Since the mean gut transit time of ingested food is about 2.5 h at 25 °C for *E. fetida* (Hartenstein & Hartenstein, 1981), we assume that most earthworms fed on the PS_{red}-spiked pellets multiple times. For subsequent experiments assessing the effects of MPP on coelomocyte viability and subpopulation distribution, non-fluorescent MPP were used instead of PS_{red} to avoid potential confounding effects of the rhodamine B label.

3.2. Linking MPP exposure to changes in earthworm weight and coelomocyte abundance and viability

Before evaluating the effects of MPP ingestion, it was studied to which extend husbandry outside soil alone has an effect on earthworm survival, coelomocyte abundance and the number of dead cells (assessed with DAPI staining). Coelomocytes were collected from earthworms incubated for 24 h in the wet chamber without food to defecate (control, n = 8) and compared to coelomocytes from earthworms exposed to food pellets without MPP for 6 days in a wet chamber (mock treatment, n = 24) to assess the effects of prolonged husbandry outside soil on earthworms and coelomocytes abundance and viability. All earthworms of the 6 day mock treatment survived, showing that prolonged husbandry outside soil is possible in our designed wet chamber and that it does not affect earthworm survival. Regarding the coelomocytes retrieved by the non-invasive isolation method, we found 82.8 ± 6.1% viable cells in the control group and 82.1 ± 9.0% in the mock treatment group (Table S2). From this we deduced that prolonged husbandry per se does also not affect the coelomocyte yield and that approximately 18% dead coelomocytes found in these experiments defines the experimental cellular mortality threshold.

Next, earthworms were given access to food pellets containing no MPP for the mock treatment and otherwise 10% PS or $PS_{Irgafos}$ for six days. Afterwards the worms were collected, weighed and coelomocytes were isolated. The earthworms' weight before (linear mixed model (lmm), X^2 =

0.843, p = 0.656) and at the end of the experiments (lmm, X^2 = 0.701, p = 0.705; Fig. S3, Table S3) showed no significant differences between individuals in the mock treatment and those in the MPP-challenge. This indicates that all groups equally fed on their respective food pellet and that ingestion of PS or $PS_{Irgafos}$ did not adversely affect their weight. On the other hand, differences were observed for the respective coelomocyte populations (Fig. 3). While the total number of isolated cells per mg fw did not differ between treatments (lmm, X^2 = 4.082, p = 0.130) (Fig. 3A), we detected a significant reduction in coelomocyte viability after PS (z = -2.347, p = 0.039) and $PS_{Irgafos}$ ingestion (z = -2.231, p = 0.039) (Fig. 3B). In addition, $PS_{Irgafos}$ ingestion also reduced the living cell count per mg fw compared to the mock group (z = -2.541, p = 0.033) (Fig. 3C).

MPP ingestion thus has an effect on earthworm immune cells rather than viability and weight gain of the actual worms. The putative immunomodulatory or cytotoxic effect on the immune cells is possibly amplified by Irgafos 168. The size range of PS and $PS_{Irgafos}$ (20 - 75 µm) used in the experiment is likely too large to enable a translocation through the intestinal tissue barrier into the earthworms' body cavity (Xiao et al., 2022), where the coelomocytes are located (Bilej et al., 2010; Cooper et al., 2002). It is thus unlikely that the observed effects result from a direct contact of the coelomocytes with PS or $PS_{Irgafos}$. Rather, the ingestion of PS or $PS_{Irgafos}$ induces a systemic sublethal stress in the earthworms, which may in turn affect coelomocyte mortality and/or enhance their sensitivity towards additional stress, e.g. during the extrusion process as potential stressor. This effect is further enhanced by the presence of Irgafos 168 leading to a significantly reduced number of viable cells per mg fresh weight compared to the mock treatment group.

To our knowledge so far, no study has analysed the effects of antioxidant additives on earthworm immune cells. However, exposure to the plastiziser di-n-butyl phthalate in soil has been shown to induce apoptosis and the activity of antioxidant defence enzymes in *E. fetida* coelomocytes (Ma et al., 2025). Irgafos 168 and di-n-butyl phthalate are both hydrophobic substances (Hermabessiere et al., 2020; Sekula et al., 2004), which makes their accumulation in tissues

possible (Hermabessiere et al., 2020; Zeng et al., 2013). Coelomocytes may thus react sensitively to substances even if the cells themselves are not directly exposed to these substances. Thus, we analysed the obtained coelomocyte population for apoptotic cells by evaluating the sub-G1 peak in DAPI stained samples (Fig. 1D). During apoptosis DNA is fragmented, resulting in cells containing a deficit DNA content ("sub-G1" Peak; Fig. 1D) (Kajstura et al., 2007). As coelomocytes isolated from worms kept for 24 h in the wet chamber (see above) did not exhibit sub-G1 peaks (<5%) in significant numbers (Table S4), we concluded that apoptosis is not induced solely due to the fact that the worms are kept outside soil for 24 h or the chosen non-invasive coelomocyte isolation procedure. On the other hand, among the 71 earthworms kept in the wet chambers for 6 d, independently of the treatment, 47 showed similar number of cells in the sub G1 population (Table S4). These findings suggest apoptosis in coelomocytes is mainly induced by sub-lethal stress caused by prolonged husbandry in a wet chamber rather than by exposure to MPP in the food.

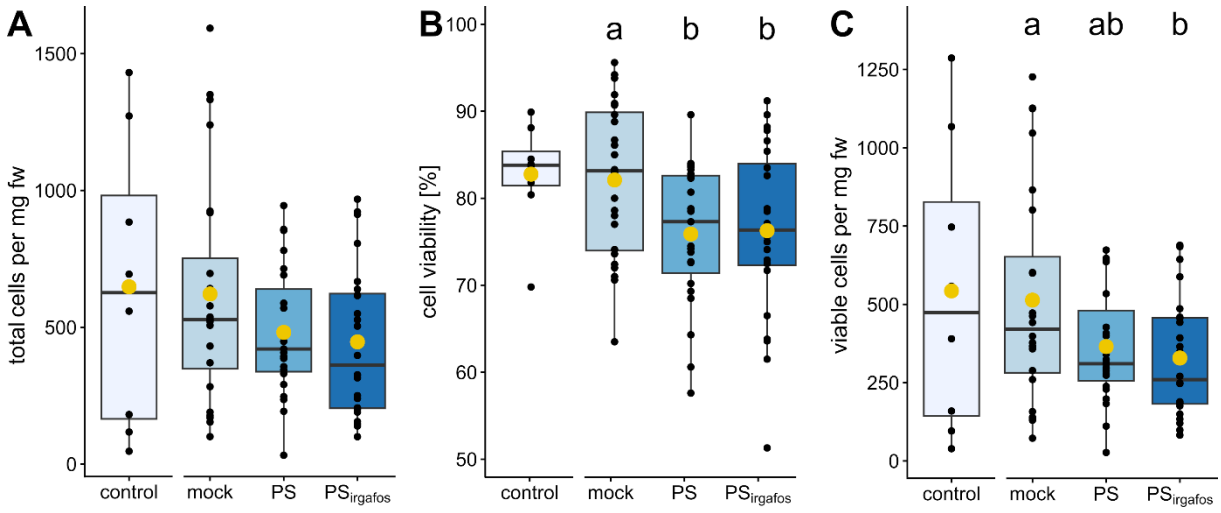

Fig. 3 Effects of MPP on coelomocyte number and viability. (A) Total number of isolated cells per mg fresh weight (fw). (B) Coelomocyte viability. (C) Different small letters indicate significant differences between treatments, determined by post-hoc Tukey comparisons. Black dots represent individual earthworms and box plots show inter-quartile range (box), median (horizontal line), mean (yellow point), and maximum/minimum of the 1.5 x interquartile ranges (whiskers). The control is not included in the statistical analysis. $n_{control} = 8$, $n_{mock} = 24$, $n_{PS} = 23$, $n_{PSIrgafos} = 24$.

3.3. Effects of MPP exposure on coelomocyte subpopulation distribution pattern

We further investigated how husbandry in a wet chamber, respectively the ingestion of PS or $PS_{Irgafos}$ affected the relative proportions of the two coelomocyte subpopulations, namely amoebocytes and eleocytes. Isolated coelomocytes were analysed by flow cytometry to quantify intrinsic riboflavin fluorescence and amounts of dead cells with DAPI staining (Fig. 1D). Riboflavin fluorescence measured in the flow cytometric measurements was divided into discrete gates: "Riboflavin^{Dim}" (fluorescence intensity 450–7K) presumed to represent amoebocytes; "Riboflavin^{Bright}" (fluorescence intensity 35K–1.5M) presumed to represent eleocytes; and "Riboflavin^{Inter}" (fluorescence intensity 7K–35K) (Fig. 4A).

Coelomocytes isolated from eight individual worms after 24 h in the wet chamber ("control") consistently exhibited a bimodal distribution of their coelomocytes' riboflavin content, assumed to correspond to the amoebocyte and eleocyte fractions (Fig. 4A middle, Fig. S4, Table S5). Coelomocyte populations isolated from worms cultivated for 6 d in the wet chamber under the different experimental conditions, on the other hand, tended to show a deviating pattern, including unimodal or trimodal fluorescence intensity patterns. The trimodal patterns typically showed an additional distinct peak at an intermediate riboflavin content (Riboflavin^{Inter}) separated from the amoebocyte (Riboflavin^{Dim}) and eleocyte populations (Riboflavin^{Bright}) (Fig. 4A, Fig. S5). We presume that this population corresponds to riboflavin depleted eleocytes. Unimodal distributions were observed with an intermediate to high riboflavin fluorescence (Fig. 4A, Fig. S5), thus presumably representing populations dominated either by healthy eleocytes or again riboflavin depleted eleocytes. Loss of riboflavin in coelomocytes fluorescence has been established as a marker for heavy metal induced stress in earthworms (Plytycz et al., 2009, 2010, 2011). Our data suggest that a loss of riboflavin, as part of a stress response, is not only a marker for heavy metal contamination, but a general stress marker, e.g. here triggered by the uptake of MPP.

The frequency of uni-, bi-, and trimodal distribution patterns showed a significant dependency on treatment (chisq test, $X^2 = 9.770$, $p = 0.044$) (Fig. 4B). In the mock treated group, 50% of the isolated coelomocyte populations still exhibited the bimodal distribution pattern, 33.3% displayed a unimodal pattern, and 16.7% a trimodal distribution pattern. In the case of PS-treated earthworms, most of the isolated coelomocyte populations displayed a trimodal distribution (10 individuals, 43.5%; mock vs. PS: chisq test, $X^2 = 7.998$, $p = 0.019$), while only one population (4.3%) had a unimodal distribution. $PS_{Irgafos}$-treated earthworms showed the highest frequency of populations with a unimodal profile (37.5%), while the frequency of the uni -, bi- and trimodal subpopulation distribution patterns remained comparable to that of the mock group (mock unimodal: 33.3%, bimodal: 50%, trimodal: 16.7%) (mock vs. $PS_{Irgafos}$: chisq test, $X^2 = 0.887$, $p = 0.754$; Fig. 4B).

Since non-bimodal distribution patterns already appeared in the mock treated group but not in the coelomocytes isolated from the control worms after 24 h, the emergence of such non-bimodal distribution patterns is likely caused *inter alia* by the husbandry conditions outside the soil. Most likely they can be considered a procedural effect, since earthworms are thin-skinned organisms with close to no protection against changes in moisture, temperature, and their chemical surroundings (Edwards & Arancon, 2022).

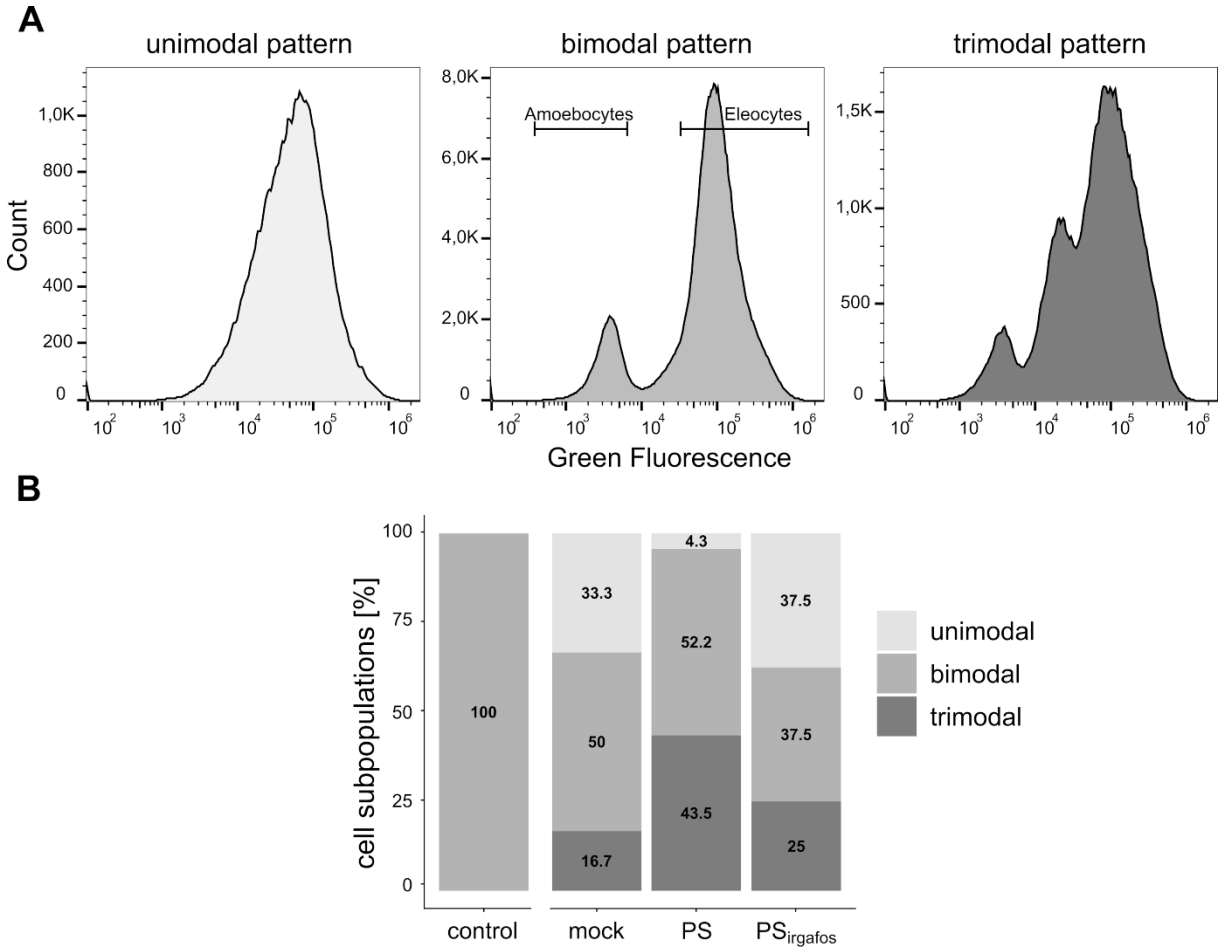

Fig. 4 Analysis of coelomocyte subpopulations after particle ingestion. (A) Flow cytometric analysis of cell subpopulations (gate "Coelomocytes") according to cell-level green autofluorescence. Uni-, bi and trimodal subpopulations distribution patterns were detected. (D) Frequency of coelomocyte subpopulations after respective treatment and frequency of coelomocyte subpopulations of earthworms kept on in wet chambers for 24 h (control). Number in the barplots represent the percentage of earthworms with the respective number of subpopulations. $n_{control}$ = 8, n_{mock} = 24, n_{PS} = 23, $n_{PSIrgafos}$ = 24.

Concomitantly, an additional specific effect can be deduced from these data for the exposure of earthworms to PS or $PS_{Irgafos}$. Coelomocytes isolated from mock treated worms showed a lower fraction of amoebocytes and a higher fraction of eleocytes than populations isolated from earthworms treated either with PS or $PS_{Irgafos}$ (Fig. 5B), even though these differences were not statistically significant (amoebocytes: lmm, $X^2 = 5.111$, $p = 0.078$, eleocytes: lmm, $X^2 = 3.625$, $p = 0.163$). Since $PS_{Irgafos}$ exposed earthworms predominantly showed a unimodal distribution pattern in the $Riboflavin^{Brigh}$-range, they had the lowest number of amoebocytes.

It is known that amoebocytes numbers are depleted after stress (Homa et al., 2016). Amoebocytes are more likely to enter the apoptotic pathway after the acute immune stimulation,

while eleocytes are more resistant (Homa et al., 2016). An immune stimulation by Irgafos 168 may thus induce apoptosis and in consequence loss of amoebocytes. When we look at the appearance of a sub G1 peak in gated eleocytes and amoebocytes subpopulation, we detected, regardless of the treatment, considerably more sub G1 cells in the amoebocyte subpopulation than in the eleocyte subpopulation (see Fig. S6, Table S6). As apoptosis progresses, cells disintegrate and are no longer measurable in flow cytometric analyses. So, prolonged exposure to $PS_{Irgafos}$, as in our 6-day feeding trial, may indeed result in a loss of the amoebocyte subpopulation and a relative increase in the eleocyte subpopulation and hence the observed shift towards a unimodal fluorescence distribution.

While the appearance of a trimodal pattern was most likely in coelomocyte populations isolated from earthworms fed with PS (Fig. S5), the proportion of coelomocytes in the intermediate population in a given trimodal distributions did not significantly differ between mock-, PS-, and $PS_{Irgafos}$-treated worms (lmm, $X^2 = 2.161$, $p = 0.340$). The likelihood of an appearance of the intermediate fraction thus depends on the experimental set up, while the relative number of cells in that fraction shows little dependency on this parameter.

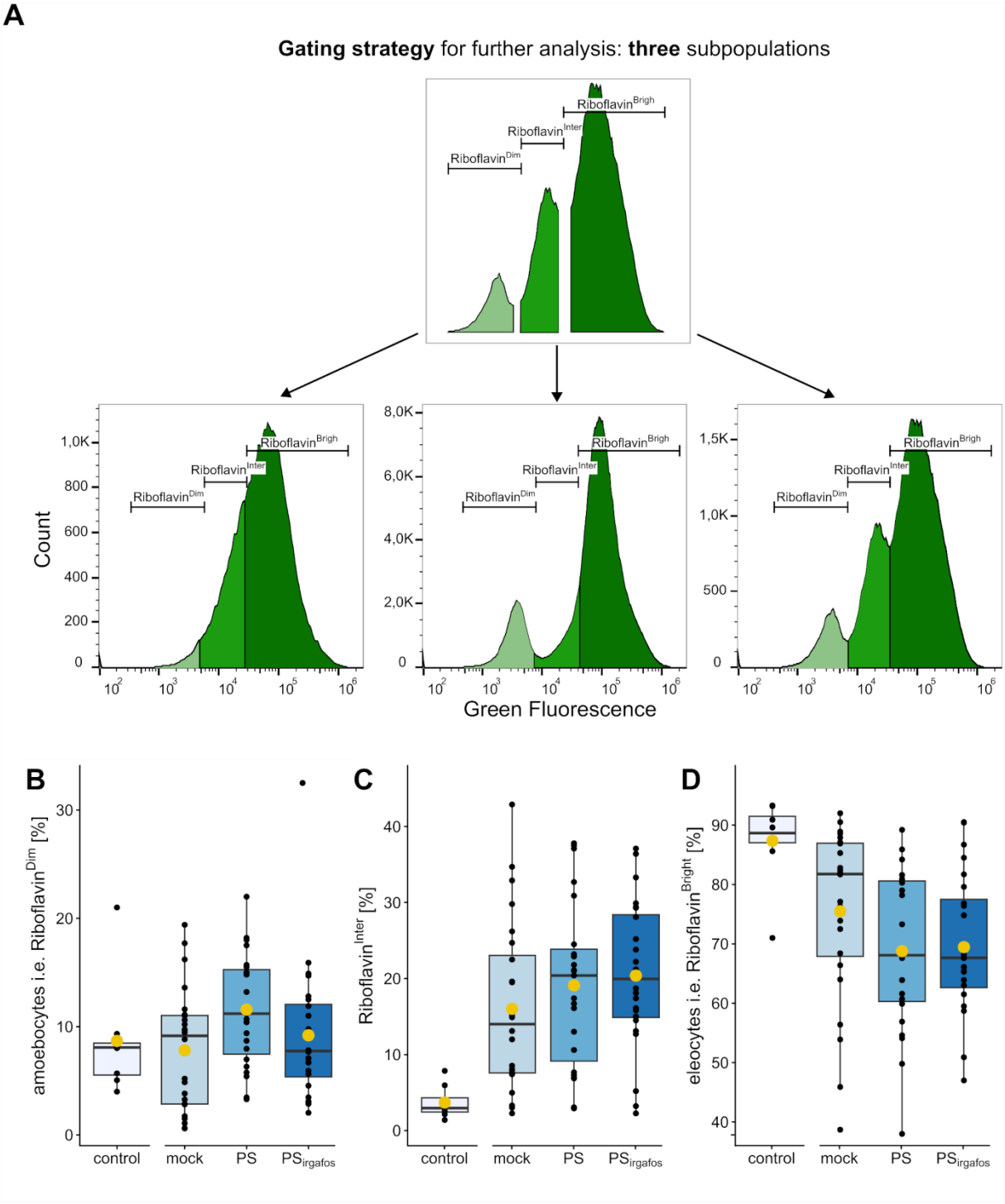

Fig. 5 Quantitative analysis of coelomocyte subpopulations of earthworms after a period of 24 h for defecation (24 h control), earthworms exposed to a food pellet for 6 days (control) or earthworms exposed to food pellet spiked with PS (PS) or $PS_{Irgafos}$ ($PS_{Irgafos}$). (A) Gating strategy for quantitative analysis of coelomocyte subpopulations (gate "coelomocytes". "$Riboflavin^{Dim}$" (fluorescence intensity 450–7K) representing amoebocytes; "$Riboflavin^{Bright}$" (fluorescence intensity 35K -1.5M) representing eleocytes and "$Riboflavin^{Inter}$" (fluorescence intensity 7K–35K (B) Effect of MPP on the frequencies of the proportion of amoebocytes, (C) intermediate population, and (D) eleocytes. Black dots represent individual earthworms and box plots show inter-quartile range (box), median (horizontal line), mean (yellow point), and maximum/minimum of the 1.5 x interquartile ranges (whiskers). The control is not included in the statistical analysis. $n_{control} = 8$, $n_{mock} = 24$, $n_{PS} = 23$, $n_{PSIrgafos} = 24$.

3.4. *Ex vivo* analysis of cell viability with MTT

The observed reduction in coelomocyte viability of the MPP-challenged worms, may arise from multiple mechanisms. The possibility of a direct cytotoxic effect of the additive Irgafos or – less likely – the MPP, has already been discussed. Alternatively, a systemic effect, whereby MPP in the gut triggers a physiological response at the organismic level cannot be excluded. Such a putative effect would indirectly compromise coelomocyte viability, without requiring direct particle-cell contact. To distinguish between these mechanisms putatively underlying MPP induced immunotoxicity in earthworms, we investigated the dose-dependent effects of PS and $PS_{Irgafos}$ in *ex vivo* assays using coelomocytes isolated from earthworms maintained in a wet chamber for 24 h for defecation. Cellular metabolic activity was quantified by the MTT assay after 24, 72, and 144 h of incubation. The 72-h time point corresponds to the average residence time of MPP in the earthworm gut following ingestion, whereas 144 h approximates the duration of the 6-day feeding regimen in the wet chamber.

Exposure to PS (Fig. 6A) in general had a mild and usually positive effect on the metabolic activity (Table S7). After 144 h, all tested MPP concentrations resulted in a significant enhancement of metabolic activity (all pairwise comparisons $p < 0.003$; Table S7). These results imply that e*x vivo* exposure to PS-MPP stimulates coelomocyte metabolic activity. A likely explanation is that PS induced a stress reaction in the coelomocytes, which subsequently lead to the observed elevated metabolic activity. Exposure to PS in soil has been shown to alter the activity of anti-oxidative enzymes (i.e., superoxide dismutase and glutathione) in earthworm tissues, indicating that the organisms up-regulate metabolic pathways to cope with the stress (Jiang et al., 2020). A separate publication showed that high LDPE doses in soil (>0.1% w/w) impaired earthworm growth and induced stress responses, mediated by excess reactive-oxygen species and thus require increased cellular energy to sustain detoxification and repair mechanisms (Y. Chen et al., 2020; Guo et al., 2023). While a direct link between MPP-induced oxidative challenges at the whole-organism and *ex vivo* MPP exposure leading to enhanced coelomocytes metabolic activity

has not been demonstrated in the pertinent literature, the shared oxidative-stress response suggests that such an increase is plausible.

In contrast, exposure to $PS_{Irgafos}$ reduced metabolic activity at all timepoints and concentrations, with the possible exception of 25 µg/mL after 72 h (Fig. 6B, Table S7). Tendentially, the effect on the metabolic activity decreases with exposure time, while there is no pronounced dependency on the concentration. The observed differences between the effect of PS-MPP and $PS_{Irgafos}$-MPP suggests that the presence of Irgafos counteracts the stimulatory effect of PS alone. Additives like Irgafos 168 are not covalently bound to the polymer matrix and can therefore leach out (Iftikhar et al., 2024). Studies about the effects of Irgafos 168 on aquatic organisms reported an adverse effect on *Daphnia magna* mobility (Marielle et al., 2018), indicating a negative effect of Irgafos 168 on invertebrates. To date, coelomocyte research has largely focussed on heavy metals, oxidative stress, and immune metabolism. Our results offer the first indication that common plastic additives such as Irgafos 168 can be toxic to earthworm coelomocytes, potentially impacting amoebocytes more strongly via the induction of apoptosis.

Finally, the question arose, whether differences in residual monomer content could also contribute to the observed phenomena. However, liquid NMR spectroscopy revealed that both materials had comparable residual monomer concentrations (0.16–0.2‰ of the MPP) (Table S1), which fall within a range that has previously been observed to be only slightly toxic in MTT assays using the reference cell line L929 (ISO 10993-5) (Zhang et al., 2023). It can therefore be assumed that it is the Irgafos itself, which contributes significantly to the observed modulation of cellular metabolic activity.

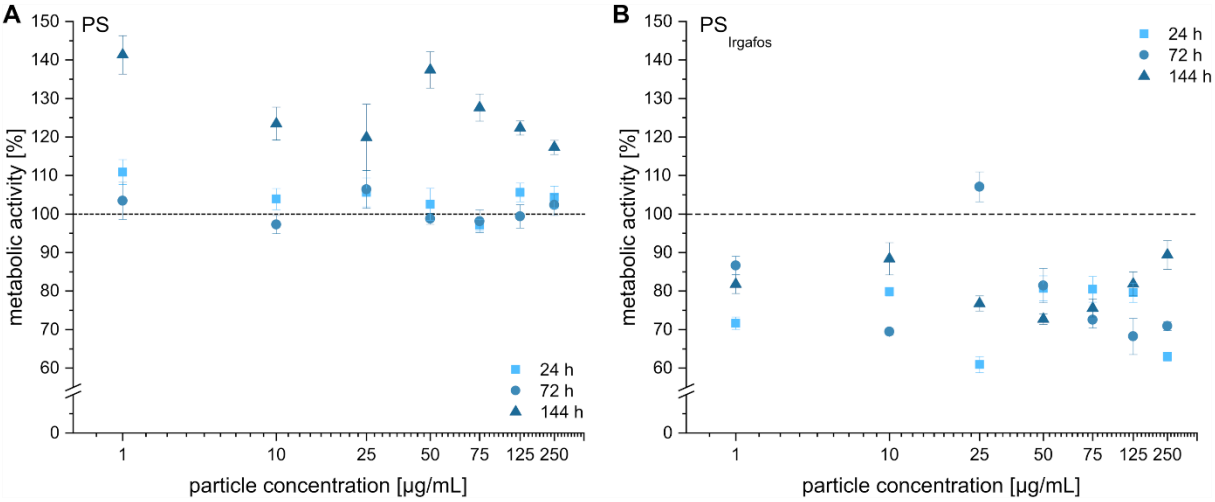

Fig. 6 Effect of microplastic on the metabolic activity of *ex vivo* coelomocytes. Effect of (A) PS and (B) $PS_{Irgafos}$ on metabolic activity after 24, 72 and 144 h incubation. Metabolic activity was analysed using the MTT assay. Cells cultivated in the absence of MPP served as negative control and their mean metabolic activity was defined as 100% (dashed line). Values are given in table S7. Data represent mean ± standard error. n ≥ 5.

4. Conclusion

In this study, we established a method for the controlled exposure of *E. fetida* to MPP-spiked food pellets. Our experimental setup ensures that earthworms actively ingest MPP, which is not achievable when earthworms are cultivated in MPP-contaminated soil. Immune cells (coelomocytes) were obtained from the earthworms in a non-invasive manner, which allowed for the first time to study the direct influence of MPP exposure through food/ intestinal passage on the worm's immune system. By further breaking down the coelomocyte fraction into the macrophage-like amoebocytes and the eleocytes involved in the humoral immune response and the detoxification of the body through their lysosomal system, we could further elucidate details in the response of the earthworm's immune system.

The size of the investigated particles, 20 to 75 µm, was considered too large for a translocation through the intestinal tissue barrier into the earthworms' body cavities. Hence an effect mediated by direct MPP-to-coelomocyte contact was unlikely. The additive Irgafos, an antioxidant commonly found in plastics, can on the other hand leach out from the MPP and can putatively directly reach the cells. While we observed no effect caused by the MPP on earthworm viability and body weight, i.e. no direct organismic effect, distinct effects on the coelomocyte

565 subpopulations could be observed. PS exposure increased the general metabolic activity of the
566 coelomocytes as evidenced by the MTT assay, while reducing the riboflavin content of a fraction
567 of the eleocytes (emergence of a third peak in the fluorescence distribution pattern). Riboflavin
568 is an immune-active molecule in eleocytes, its intrinsic fluorescence has been suggested as a
569 functional marker for stress-induced cellular responses. Exposure to $PS_{Irgafos}$-MPP on the other
570 hand, significantly lowered the metabolic activity of the coelomocytes, while reducing the
571 amoebocyte count in many cases down to a level, where the fluorescence distribution showed a
572 single peak corresponding to the eleocytes. While the effect of PS thus can be explained by a
573 stress reaction, $PS_{Irgafos}$ in addition seems to exert a cytotoxic effect, which is known to affect
574 amoebocytes more severely than eleocytes. Interestingly the effect of both types of MPP on the
575 metabolic activity showed neither a time nor a concentration dependence.
576 Our work gives the first insights on how MPP and common plastic additives found therein may
577 perturb the earthworm's immune system. In future this may help to correlate the effects of
578 certain contaminants on earthworm immune cells with their chemical structures thereby
579 supporting the classification of such molecules for ecological risk evaluation. This can ultimately
580 lead to safer-by-design strategies for polymer formulation ultimately reducing the environmental
581 and biological risks of plastic leachates.

Statements and Declarations

Funding

This study was funded by the Deutsche Forschungsgemeinschaft (DFG, German Research Foundation)– Project-ID 391977956 – SFB 1357

Data availability

All data and R code have been submitted with the manuscript and will be made publicly available on GitHub and Zenodo upon acceptance.

Competing Interests

The authors have no competing interests to declare that are relevant to the content of this article.

References

Adamowicz, A., & Wojtaszek, J. (2001). Morphology and phagocytotic activity of coelomocytes in Dendrobaena veneta (Lumbricidae). *Tissue and Cell*, *46*, 125–133. https://doi.org/10.1016/j.tice.2004.11.002

Atale, N., Gupta, S., Yadav, U. C. S., & Rani, V. (2014). Cell-death assessment by fluorescent and nonfluorescent cytosolic and nuclear staining techniques. *Journal of Microscopy*, *255*(1), 7–19. https://doi.org/10.1111/jmi.12133

Bates, D., Mächler, M., Bolker, B., & Walker, S. (2015). Fitting Linear Mixed-Effects Models Using **lme4**. *Journal of Statistical Software*, *67*(1). https://doi.org/10.18637/jss.v067.i01

Bilej, M., Procházková, P., Šilerová, M., & Josková, R. (2010). Earthworm immunity. In K. Söderhäll (Ed.), *Invertebrate Immunity* (Vol. 708, pp. 66–79). Springer US. https://doi.org/10.1007/978-1-4419-8059-5_4

Blouin, M., Hodson, M. E., Delgado, E. A., Baker, G., Brussaard, L., Butt, K. R., Dai, J., Dendooven, L., Peres, G., Tondoh, J. E., Cluzeau, D., & Brun, J.-J. (2013). A review of earthworm impact on soil function and ecosystem services. *European Journal of Soil Science*, *64*(2), 161–182. https://doi.org/10.1111/ejss.12025

Bodó, K., Ernszt, D., Németh, P., & Engelmann, P. (2018). Distinct immune- and defense-related molecular fingerprints in sepatated coelomocyte subsets of Eisenia andrei earthworms. *Invertebrate Survival Journal*, *Vol. 15 No. 1 2018*.

Chen, K., Tang, R., Luo, Y., Chen, Y., Ei-Naggar, A., Du, J., Bu, A., Yan, Y., Lu, X., Cai, Y., & Chang, S. X. (2022). Transcriptomic and metabolic responses of earthworms to contaminated soil with polypropylene and polyethylene microplastics at environmentally relevant concentrations. *Journal of Hazardous Materials*, *427*, 128176. https://doi.org/10.1016/j.jhazmat.2021.128176

Chen, Y., Chen, Q., Zhang, Q., Zuo, C., & Shi, H. (2022). An overview of chemical additives on (micro)plastic fibers: Occurrence, release, and health risks. *Reviews of Environmental Contamination and Toxicology*, *260*(1), 22. https://doi.org/10.1007/s44169-022-00023-9

Chen, Y., Liu, X., Leng, Y., & Wang, J. (2020). Defense responses in earthworms (Eisenia fetida) exposed to low-density polyethylene microplastics in soils. *Ecotoxicology and Environmental Safety*, *187*, 109788. https://doi.org/10.1016/j.ecoenv.2019.109788

Cooper, E. L., Beschin, A., & Bilej, M. (Eds). (2002). *A new model for analyzing antimicrobial peptides with biomedical applications*. NATO Advanced Research Workshop on a New Model for Analyzing Antimicrobial Peptides with Biomedical Applications, Amsterdam ; Washington, DC. IOS Press.

DIN EN ISO 24187:2024-04, Grundsätze für die Analyse von Mikroplastik in der Umwelt (ISO_24187:2023); Deutsche Fassung EN_ISO_24187:2023. (2024). DIN Media GmbH. https://doi.org/10.31030/3495706

631 Dinno, A. (2024). *dunn.test: Dunn's test of multiple comparisons using rank sums* (Version
632 1.3.6) [Computer software]. https://cran.r-
633 project.org/web/packages/dunn.test/index.html
634 Du, L., Wu, A., Liu, G., Li, H., Yu, B., Zhen, H., & Wang, X. (2020). Green autofluorescence
635 eleocytes from earthworm as a tool for detecting environmental iron pollution.
636 *Ecological Indicators*, *108*, 105695. https://doi.org/10.1016/j.ecolind.2019.105695
637 Earth Action. (2023). *Leakage of microplastics into oceans and land*.
638 Edwards, C. A., & Arancon, N. Q. (2022). *Biology and ecology of earthworms*. Springer US.
639 https://doi.org/10.1007/978-0-387-74943-3
640 Engelmann, P., Hayashi, Y., Bodó, K., Ernszt, D., Somogyi, I., Steib, A., Orbán, J., Pollák,
641 E., Nyitrai, M., Németh, P., & Molnár, L. (2016). Phenotypic and functional
642 characterization of earthworm coelomocyte subsets: Linking light scatter-based cell
643 typing and imaging of the sorted populations. *Developmental & Comparative*
644 *Immunology*, *65*, 41–52. https://doi.org/10.1016/j.dci.2016.06.017
645 Engelmann, P., Pál, J., Berki, T., Cooper, E. L., & Németh, P. (2002). Earthworm leukocytes
646 react with different mammalian antigen-specific monoclonal antibodies. *Zoology*,
647 *105*(3), 257–265. https://doi.org/10.1078/0944-2006-00068
648 Eyambe, G. S., Goven, A. J., Fitzpatrick, L. C., Venables, B. J., & Cooper, E. L. (1991). A
649 non-invasive technique for sequential collection of earthworm (*Lumbricus terrestris*)
650 leukocytes during subchronic immunotoxicity studies. *Laboratory Animals*, *25*(1), 61–
651 67. https://doi.org/10.1258/002367791780808095
652 Fox, J., & Weisberg, S. (2019). *An R companion to applied regression (third edition)*. Sage.
653 https://socialsciences.mcmaster.ca/jfox/Books/Companion/
654 Guo, S., Wang, Q., Li, Z., Chen, Y., Li, H., Zhang, J., Wang, X., Liu, J., Cao, B., Zou, G.,
655 Zhang, B., & Zhao, M. (2023). Ecological risk of microplastic toxicity to earthworms in
656 soil: A bibliometric analysis. *Frontiers in Environmental Science*, *11*.
657 https://doi.org/10.3389/fenvs.2023.1126847

Hartenstein, R., & Hartenstein, F. (1981). Physicochemical changes effected in activated sludge by the earthworm Eisenia foetida. *Journal of Environmental Quality*, *10*(3), 377–381. https://doi.org/10.2134/jeq1981.00472425001000030027x

Hartig, F. (2022). *DHARMa: Residual diagnostics for hierarchical (multi-level/mixed) regression models.* [Computer software]. https://CRAN.R-project.org/package=DHARMa.

Hermabessiere, L., Receveur, J., Himber, C., Mazurais, D., Huvet, A., Lagarde, F., Lambert, C., Paul-Pont, I., Dehaut, A., Jezequel, R., Soudant, P., & Duflos, G. (2020). An Irgafos® 168 story: When the ubiquity of an additive prevents studying its leaching from plastics. *Science of The Total Environment*, *749*, 141651. https://doi.org/10.1016/j.scitotenv.2020.141651

Holzinger, A., Hink, L., Sehl, E., Rüppel, N., Lehndorff, E., Weig, A. R., Agarwal, S., Horn, M. A., & Feldhaar, H. (2023). Biodegradable polymers boost reproduction in the earthworm Eisenia fetida. *Science of The Total Environment*, *892*, 164670. https://doi.org/10.1016/j.scitotenv.2023.164670

Homa, J., Bzowska, M., Klimek, M., & Plytycz, B. (2008). Flow cytometric quantification of proliferating coelomocytes non-invasively retrieved from the earthworm, Dendrobaena veneta. *Developmental & Comparative Immunology*, *32*(1), 9–14. https://doi.org/10.1016/j.dci.2007.04.007

Homa, J., Stalmach, M., Wilczek, G., & Kolaczkowska, E. (2016). Effective activation of antioxidant system by immune-relevant factors reversely correlates with apoptosis of Eisenia andrei coelomocytes. *Journal of Comparative Physiology B*, *186*(4), 417–430. https://doi.org/10.1007/s00360-016-0973-5

Homa, J., Zorska, A., Wesolowski, D., & Chadzinska, M. (2013). Dermal exposure to immunostimulants induces changes in activity and proliferation of coelomocytes of Eisenia andrei. *Journal of Comparative Physiology B*, *183*(3), 313–322. https://doi.org/10.1007/s00360-012-0710-7

Horton, A. A., Walton, A., Spurgeon, D. J., Lahive, E., & Svendsen, C. (2017). Microplastics in freshwater and terrestrial environments: Evaluating the current understanding to identify the knowledge gaps and future research priorities. *Science of The Total Environment*, *586*, 127–141. https://doi.org/10.1016/j.scitotenv.2017.01.190

Hothorn, T., Bretz, F., & Westfall, P. (2008). Simultaneous inference in general parametric models. *Biometrical Journal*, *50*(3), 346–363. https://doi.org/10.1002/bimj.200810425

Iftikhar, A., Qaiser, Z., Sarfraz, W., Ejaz, U., Aqeel, M., Rizvi, Z. F., & Khalid, N. (2024). Understanding the leaching of plastic additives and subsequent risks to ecosystems. *Water Emerging Contaminants & Nanoplastics*, *3*(1). https://doi.org/10.20517/wecn.2023.58

Irizar, A., Duarte, D., Guilhermino, L., Marigómez, I., & Soto, M. (2014). Optimization of NRU assay in primary cultures of Eisenia fetida for metal toxicity assessment. *Ecotoxicology*, *23*(7), 1326–1335. https://doi.org/10.1007/s10646-014-1275-x

Jiang, X., Chang, Y., Zhang, T., Qiao, Y., Klobučar, G., & Li, M. (2020). Toxicological effects of polystyrene microplastics on earthworm (Eisenia fetida). *Environmental Pollution*, *259*, 113896. https://doi.org/10.1016/j.envpol.2019.113896

Kajstura, M., Halicka, H. D., Pryjma, J., & Darzynkiewicz, Z. (2007). Discontinuous fragmentation of nuclear DNA during apoptosis revealed by discrete “sub-G1” peaks on DNA content histograms. *Cytometry Part A*, *71A*(3), 125–131. https://doi.org/10.1002/cyto.a.20357

Kassambara, A. (2023). *ggpubr: ‘Ggplot2’ Based Publication Ready Plots* [Computer software]. https://cran.r-project.org/web/packages/ggpubr/index.html

Kedzierski, M., Cirederf-Boulant, D., Palazot, M., Yvin, M., & Bruzaud, S. (2023). Continents of plastics: An estimate of the stock of microplastics in agricultural soils. *Science of The Total Environment*, *880*, 163294. https://doi.org/10.1016/j.scitotenv.2023.163294

Koziol, B., Markowicz, M., Kruk, J., & Plytycz, B. (2006). Riboflavin as a source of autofluorescence in Eisenia fetida coelomocytes. *Photochemistry and Photobiology*, *82*(2), 570. https://doi.org/10.1562/2005-11-23-RA-738

713 Kühn, S., & Van Franeker, J. A. (2020). Quantitative overview of marine debris ingested by
714 marine megafauna. *Marine Pollution Bulletin*, *151*, 110858.
715 https://doi.org/10.1016/j.marpolbul.2019.110858
716 Kurek, A., Homa, J., Kauschke, E., & Plytycz, B. (2007). Characteristics of coelomocytes of
717 the stubby earthworm, Allolobophora chlorotica (Sav.). *European Journal of Soil*
718 *Biology*, *43*, S121–S126. https://doi.org/10.1016/j.ejsobi.2007.08.051
719 Li, B., Lan, Z., Wang, L., Sun, H., Yao, Y., Zhang, K., & Zhu, L. (2019). The release and
720 earthworm bioaccumulation of endogenous hexabromocyclododecanes (HBCDDs)
721 from expanded polystyrene foam microparticles. *Environmental Pollution*, *255*,
722 113163. https://doi.org/10.1016/j.envpol.2019.113163
723 Liu, J., Qin, J., Zhu, L., Zhu, K., Liu, Z., Jia, H., & Lichtfouse, E. (2022). The protective layer
724 formed by soil particles on plastics decreases the toxicity of polystyrene microplastics
725 to earthworms (Eisenia fetida). *Environment International*, *162*, 107158.
726 https://doi.org/10.1016/j.envint.2022.107158
727 Liu, M., Feng, J., Shen, Y., & Zhu, B. (2023). Microplastics effects on soil biota are
728 dependent on their properties: A meta-analysis. *Soil Biology and Biochemistry*, *178*,
729 108940. https://doi.org/10.1016/j.soilbio.2023.108940
730 Lozano, Y. M., Aguilar-Trigueros, C. A., Onandia, G., Maaß, S., Zhao, T., & Rillig, M. C.
731 (2021). Effects of microplastics and drought on soil ecosystem functions and
732 multifunctionality. *Journal of Applied Ecology*, *58*(5), 988–996.
733 https://doi.org/10.1111/1365-2664.13839
734 Ma, J., Ladd, D. M., Kaval, N., & Wang, H.-S. (2025). Toxicity of long term exposure to low
735 dose polystyrene microplastics and nanoplastics in human iPSC-derived
736 cardiomyocytes. *Food and Chemical Toxicology*, *202*, 115489.
737 https://doi.org/10.1016/j.fct.2025.115489
738 Manna, S., Ray, A., Gautam, A., Mukherjee, S., Ray, M., & Ray, S. (2022). A comparative
739 account of coelomocyte of earthworm ecotypes with reference to its morphology,

morphometry, density, phagocytosis, autofluorescence, and oxidative status. *Journal of Morphology*, *283*(7), 956–972. https://doi.org/10.1002/jmor.21483

Marielle, G. M., Durrieu, C., Guenne, A., Rouillac, L., Diafi, D., Nour, I., Mazéas, L., Nathalie, T. F., & Farcas, F. (2018). Impact of polyethylene and polypropylene geomembranes in sensitive aquatic environment. *Ecotoxicology and Environmental Safety*, *148*, 884–891. https://doi.org/10.1016/j.ecoenv.2017.11.015

Mazur, A. I., Klimek, M., Morgan, A. J., & Plytycz, B. (2011). Riboflavin storage in earthworm chloragocytes and chloragocyte-derived eleocytes and its putative role as chemoattractant for immunocompetent cells. *Pedobiologia*, *54*, S37–S42. https://doi.org/10.1016/j.pedobi.2011.09.008

Papazlatani, C., Garbeva, P., & Huerta Lwanga, E. (2024). Effect of microplastic pollution on the gut microbiome of anecic and endogeic earthworms. *FEMS Microbiology Letters*, *371*, fnae040. https://doi.org/10.1093/femsle/fnae040

Plytycz, B., Kielbasa, E., Grebosz, A., Duchnowski, M., & Morgan, A. J. (2010). Riboflavin mobilization from eleocyte stores in the earthworm Dendrodrilus rubidus inhabiting aerially-contaminated Ni smelter soil. *Chemosphere*, *81*(2), 199–205. https://doi.org/10.1016/j.chemosphere.2010.06.056

Plytycz, B., Klimek, M., Klimek, B. A., Szymanski, W., Kruk, J., & Morgan, A. J. (2011). Riboflavin content in the coelomocytes of contrasting earthworm species is differentially affected by edaphic variables including organic matter and metal content. *Pedobiologia*, *54*, S43–S48. https://doi.org/10.1016/j.pedobi.2011.07.003

Plytycz, B., Lis-Molenda, U., Cygal, M., Kielbasa, E., Grebosz, A., Duchnowski, M., Andre, J., & Morgan, A. J. (2009). Riboflavin content of coelomocytes in earthworm (Dendrodrilus rubidus) field populations as a molecular biomarker of soil metal pollution. *Environmental Pollution*, *157*(11), 3042–3050. https://doi.org/10.1016/j.envpol.2009.05.046

766 Qiu, Y., Zhou, S., Zhang, C., Zhou, Y., & Qin, W. (2022). Soil microplastic characteristics
767 and the effects on soil properties and biota: A systematic review and meta-analysis.
768 *Environmental Pollution*, *313*, 120183. https://doi.org/10.1016/j.envpol.2022.120183
769 R Core Team. (2023). *R: A Language and Environment for Statistical Computing* [Computer
770 software]. https://www.R-project.org/
771 Reay, M. K., Graf, M., Murphy, M., Li, G., Yan, C., Bhattacharya, M., Osbahr, H., Ma, J.,
772 Chengtao, W., Shi, X., Ren, S., Cui, J., Collins, C., Chadwick, D., Jones, D. L.,
773 Evershed, R. P., & Lloyd, C. E. M. (2025). Higher potential leaching of inorganic and
774 organic additives from biodegradable compared to conventional agricultural plastic
775 mulch film. *Journal of Hazardous Materials*, *488*, 137147.
776 https://doi.org/10.1016/j.jhazmat.2025.137147
777 Riedl, S. A. B., Völkl, M., Holzinger, A., Jasinski, J., Jérôme, V., Scheibel, T., Feldhaar, H., &
778 Freitag, R. (2021). In vitro cultivation of primary intestinal cells from Eisenia fetida as
779 basis for ecotoxicological studies. *Ecotoxicology*, *31*(2), 221–233.
780 https://doi.org/10.1007/s10646-021-02495-2
781 Santos, R. G., Machovsky-Capuska, G. E., & Andrades, R. (2021). Plastic ingestion as an
782 evolutionary trap: Toward a holistic understanding. *Science*, *373*(6550), 56–60.
783 https://doi.org/10.1126/science.abh0945
784 Sauvat, A., Wang, Y., Segura, F., Spaggiari, S., Müller, K., Zhou, H., Galluzzi, L., Kepp, O.,
785 & Kroemer, G. (2015). Quantification of cellular viability by automated microscopy
786 and flow cytometry. *Oncotarget*, *6*(11), 9467–9475.
787 https://doi.org/10.18632/oncotarget.3266
788 Sekula, M., Pawlus, S., Hensel-Bielowka, S., Ziolo, J., Paluch, M., & Roland, C. M. (2004).
789 Structural and Secondary Relaxations in Supercooled Di-n-butyl Phthalate and
790 Diisobutyl Phthalate at Elevated Pressure. *The Journal of Physical Chemistry B*,
791 *108*(16), 4997–5003. https://doi.org/10.1021/jp0376121

792 Shi, H., Wang, Y., Li, X., Wang, X., Qi, Y., Hu, S., & Liu, R. (2024). Polystyrene nanoplastics
793 elicit multiple responses in immune cells of the Eisenia fetida (Savigny, 1826).
794 *Toxics*, *13*(1), 18. https://doi.org/10.3390/toxics13010018
795 van Oers, L., van der Voet, E., & Grundmann, V. (2012). Additives in the plastics industry. In
796 B. Bilitewski, R. M. Darbra, & D. Barceló (Eds), *Global Risk-Based Management of*
797 *Chemical Additives I: Production, Usage and Environmental Occurrence* (pp. 133–
798 149). Springer Berlin Heidelberg. https://doi.org/10.1007/698_2011_112
799 Wickham, H. (2016). *ggplot2: Elegant Graphics for Data Analysis* [Computer software].
800 Springer-Verlag. https://ggplot2.tidyverse.org
801 Wickham, H., François, R., Henry, L., Müller, K., & Vaughan, D. (2023). *dplyr: A Grammar of*
802 *Data Manipulation* [Computer software]. https://cran.r-
803 project.org/web/packages/dplyr/index.html
804 Xiao, X., He, E., Jiang, X., Li, X., Yang, W., Ruan, J., Zhao, C., Qiu, R., & Tang, Y. (2022).
805 Visualizing and assessing the size-dependent oral uptake, tissue distribution, and
806 detrimental effect of polystyrene microplastics in Eisenia fetida. *Environmental*
807 *Pollution*, *306*, 119436. https://doi.org/10.1016/j.envpol.2022.119436
808 Xue, Y., Gu, X., Wang, X., Sun, C., Xu, X., Sun, J., & Zhang, B. (2009). The hydroxyl radical
809 generation and oxidative stress for the earthworm Eisenia fetida exposed to
810 tetrabromobisphenol A. *Ecotoxicology*, *18*(6), 693–699.
811 https://doi.org/10.1007/s10646-009-0333-2
812 Yang, X., Zhang, X., Shu, X., Gong, J., Yang, J., Li, B., Lin, J., Chai, Y., & Liu, J. (2023). The
813 effects of polyethylene microplastics on the growth, reproduction, metabolic
814 enzymes, and metabolomics of earthworms *Eisenia fetida*. *Ecotoxicology and*
815 *Environmental Safety*, *263*, 115390. https://doi.org/10.1016/j.ecoenv.2023.115390
816 Zeng, Q., Wei, C., Wu, Y., Li, K., Ding, S., Yuan, J., Yang, X., & Chen, M. (2013). Approach
817 to distribution and accumulation of dibutyl phthalate in rats by immunoassay. *Food*
818 *and Chemical Toxicology*, *56*, 18–27. https://doi.org/10.1016/j.fct.2013.01.045

819 Zhang, Y., Paul, T., Brehm, J., Völkl, M., Jérôme, V., Freitag, R., Laforsch, C., & Greiner, A.
820 (2023). Role of Residual Monomers in the Manifestation of (Cyto)toxicity by
821 Polystyrene Microplastic Model Particles. *Environmental Science & Technology*,
822 *57*(27), 9925–9933. https://doi.org/10.1021/acs.est.3c01134
823
824